

## REVIEW

# A Review on Solid-State Li-S Battery: From the Conversion Mechanism of Sulfur to Engineering Design

Huan-Huan Jia<sup>a</sup>, Chen-Ji Hu<sup>a</sup>, Yi-Xiao Zhang<sup>a</sup>, Li-Wei Chen<sup>a,b,c,\*</sup>

<sup>a</sup> School of Chemistry and Chemical Engineering, Frontiers Science Center for Transformative Molecules, Shanghai Electrochemical Energy Device Research Center (SEED) and in-situ Center for Physical Sciences, Shanghai Jiao Tong University, Shanghai, 200240, PR China

<sup>b</sup> Future Battery Research Center, Global Institute of Future Technology, Shanghai Jiao Tong University, Shanghai, 200240, PR China

<sup>c</sup> i-Lab, Suzhou Institute of Nano-Tech and Nano-Bionics (SINANO), Chinese Academy of Sciences, Suzhou, 215123, PR China

## Abstract

Lithium-sulfur (Li-S) batteries attract sustained attention because of their ultrahigh theoretical energy density of 2567 Wh·kg<sup>-1</sup> and the actual value over 600 Wh·kg<sup>-1</sup>. Solid-state Li-S batteries (SSLSBs) emerge in the recent two decades because of the enhanced safety when compared to the liquid system. As for the SSLSBs, except for the difference in the conversion mechanism induced by the cathode materials themselves, the physical-chemical property of solid electrolytes (SEs) also significantly affects their electrochemical behaviors. On account of various reported Li-S batteries, the advantages and disadvantages in performance and the failure mechanism are discussed in this review. Based on the problems of the reported SSLSBs such as lower energy density and faster capacity fading, the strategies of building high-performance SSLSBs are classified. The review aims to afford fundamental understanding on the conversion mechanism of sulfur and engineering design at full-cell level, so as to promote the development of SSLSBs.

**Keywords:** Solid-state Li-S batteries; Conversion kinetics; Dynamically stable interface; Failure mechanism; Engineering design

## 1. Introduction

Lithium sulfur (Li-S) batteries have attracted sustained attention since 1960s because of their high theoretical energy density (2576 Wh·kg<sup>-1</sup>), as well as the abundant reserves, low cost and environment-friendly characteristics of sulfur [1–3]. While the sulfur-based cathode materials typically have disadvantages such as poor electronic conductivity, large volume change and the polysulfide shuttle effect, recent efforts adopting innovative material design in combination with the usage of special electrolyte additives have brought the energy density of Li-S full-cell batteries to the range of 200–400 Wh·kg<sup>-1</sup>, with some exceptional cases even exceeding 600 Wh·kg<sup>-1</sup> in pouch cells [2]. In contrast with the energy densities at the range of

100–200 Wh·kg<sup>-1</sup> for typical Li-ion batteries based on traditional intercalation cathodes, Li-S battery is considered as a promising candidate for next generation high-energy battery systems [4]. However, poor cycling performance and potential safety hazards caused by combined usage of Li metal anode and organic liquid electrolytes have hindered practical application of Li-S battery. Therefore, SSLSBs, in which organic liquid electrolytes are replaced with SEs, have emerged as a critical direction hoping for suppressed polysulfide shuttling, enhanced Li anode reversibility and improved safety performance [5–8].

Solidification of Li-S batteries greatly alters the kinetic feature of the conversion reactions in the electrodes and thus introduces unique challenges in full exploration on the potential of Li-S systems

Received 19 September 2022; Received in revised form 10 October 2022; Accepted 4 November 2022  
Available online 7 November 2022

\* Corresponding author, Liwei Chen, Tel: (86-21)54743179, E-mail address: lwchen2018@sjtu.edu.cn.

<https://doi.org/10.13208/j.electrochem.2217008>

1006-3471/© 2023 Xiamen University and Chinese Chemical Society. This is an open access article under the CC BY-NC license (<http://creativecommons.org/licenses/by-nc/4.0/>).

[6,9,10]. There is still a long way to go for both fundamental research and practical application.

This review summarizes the current exploration of SSLSBs. With the majority of current research emphasizing the engineering design and device failure mechanism, special attention is given to the chemical and electrochemical reaction mechanisms during charge/discharge processes as well as their implication in future design of SSLSBs. Specifically, an overview of SEs and the corresponding applications, and the electrode materials in SSLSBs are given in Section 2. Reported SSLSBs are classified into four categories based on the electrolyte materials used in the cell. Key challenges in two major categories, namely, SSLSBs with solid polymer electrolytes or composite solid electrolytes and SSLSBs with sulfide-based inorganic solid electrolytes, are identified. And potential solutions to these challenges are discussed in Sections 3 and 4, respectively. Finally, in Section 5, the achieved performances of SSLSBs in current reports are compared at both the half-cell and full-cell levels, and future development directions are discussed.

## 2. Overview of the materials used in SSLSBs

*Electrolyte.* In the recent two decades, SEs such as inorganic solid electrolytes (ISEs, including oxide-, sulfide- and halide-based ISEs), solid polymer electrolytes (SPEs), organic-inorganic composite solid electrolytes (CSEs) and open-framework-related composite electrolytes (MOFs-, COFs- and POCs-based SEs) have been developed and extensively investigated [11–17]. The room temperature ionic conductivity of these SEs ranges from  $10^{-5}$  S·cm<sup>-1</sup> to  $10^{-2}$  S·cm<sup>-1</sup>. These materials are fundamentally important for the development of solid-state batteries.

Among all types of SEs, ISEs have advantages of high room temperature ionic conductivities, but often suffer from high interface impedance due to poor solid-solid contacts, especially in oxide-based ISEs. While polymer-based SPEs and CSEs are mechanically compatible with existing battery assembling procedures but their room temperature ionic conductivities are often nonideal [17].

The incorporation of SEs in Li-S batteries brings profound changes to the electrode reaction kinetics [9]. The use of oxide-based ISEs supposedly prevents polysulfides shuttling. The use of sulfide-based ISEs may even change the conversion reaction mechanism of the sulfur cathode, ultimately eliminating the generation of polysulfides, and thus significantly improve the utilization of active sulfur materials [18]. However, other aspects of the

material such as ionic conductivity, chemical and electrochemical compatibility, and solid-solid contacts also need to be evaluated comprehensively for the application in solid-state systems. To this end, different SEs are often used together in a particular device to achieve balanced and hence better overall performance.

In addition to the well-known differences in electrolytes, differences also lie in the selection of cathode and anode materials for SSLSBs.

*Cathode.* The inorganic sulfur cathodes such as S/C cathodes represented by S-CMK-3, Li<sub>2</sub>S cathodes, and organic sulfur cathodes represented by SPAN are widely used in the liquid Li-S battery system [5]. However, solid-state Li-S batteries that so far have been reported mainly used inorganic sulfur or transition metal sulfide cathode materials (TiS<sub>2</sub>, MoS<sub>2</sub> etc.) [19–31]. It is noticed that very few works are reported with organic sulfur cathodes in SSLSBs, so the following discussion in this review is mainly based on inorganic sulfur cathodes, and some cases related to the organic sulfur cathodes are discussed in the perspective section.

*Anode.* Lithium metal is considered the ultimate negative electrode to realize high energy density. It is electrochemically stable against the SPEs, CSEs and oxide-based ISEs within the working voltage range. When lithium metal is coupled with oxide-based ISEs, an interlayer needs to be built between the electrode and electrolyte for reducing the huge interface impedance. This interlayer also determines the electrochemical stability of the SE layer. In most cases, lithium metal is unstable against sulfide-based ISEs because of the limited electrochemical window, hence an interlayer is needed in this case to ensure the electrochemical stability [18,32,33]. Besides, lithium-alloy anodes such as Li-In alloy, Li-Si alloy and Li-Al alloy are used in SSLSBs with sulfide-based ISEs [25,34,35].

Based on the survey described above, currently reported SSLSBs are categorized into four types based on materials used therein.

(1) Li-S batteries with SPEs (Fig. 1a), in which SPEs consisted of polymer matrix and lithium salts are used to assemble SSLSBs [36].

(2) Li-S batteries with CSEs (Fig. 1c), in which CSEs are used as SE separator and cathode additive for SSLSBs [37]. The inorganic component in CSEs contributes to the ionic conductivity and mechanical strength, while the flexible polymer component ensures effective solid-solid contact.

While the SPE and CPEs used in these two types of cells have much in common in terms of ion conduction mechanisms, their structural differences lead to separate optimization strategies for

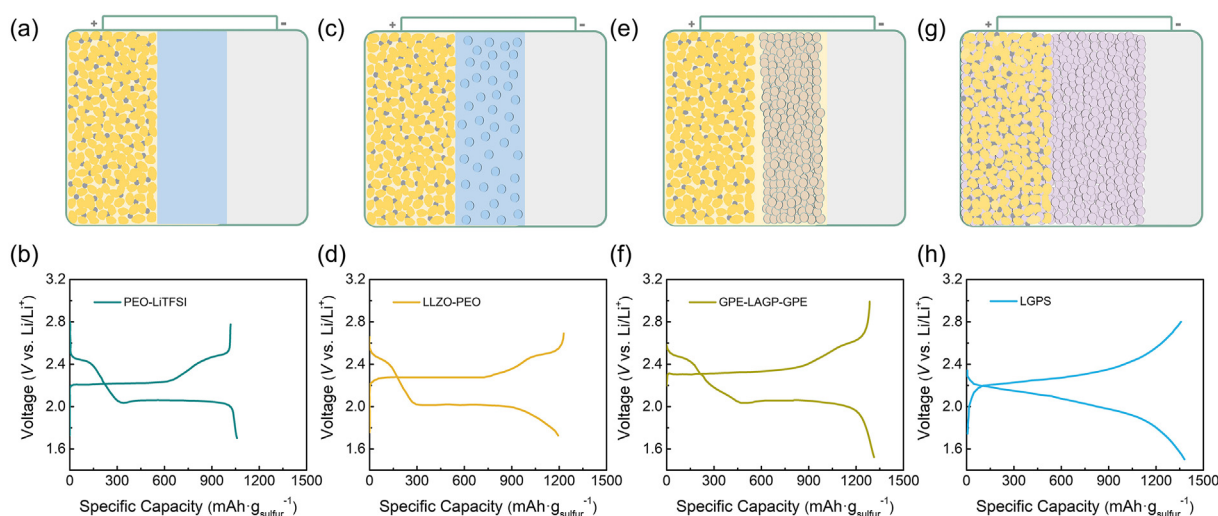


Fig. 1. Four types of currently developed SSLSBs and the corresponding galvanostatic charging/discharging curves. (a) and (b), Li-S batteries with SPEs [36]; (c) and (d), Li-S batteries with CSEs [37]; (e) and (f), Li-S batteries with oxide-based ISEs as separator with interfacial wetting layers [38]; (g) and (h), Li-S batteries with sulfide-based ISEs [18]. The data in (b), (d), (f) and (h) are digitized from Ref. [36], Ref. [37], Ref. [38] and Ref. [18], respectively.

application in Li-S cells. For example, the selection of lithium salt is often employed in regulating the properties in SPEs. In addition, the inorganic component in CSEs is an extra dimension of variability that is not available for SPEs.

(3) Li-S batteries with oxide-based ISEs separator and interfacial wetting layers (Fig. 1e) [38]. In this type of cells, a dense ceramic electrolyte layer with high ion conductivities can transport Li-ions and block lithium dendrite growth, while the interfacial wetting layer is used to improve contact and lower the interfacial impedance.

(4) Li-S batteries with sulfide-based ISEs (Fig. 1g) [18]. Sulfide solid electrolytes are relatively soft in comparison to oxide ceramic electrolytes, and thus are often used as both the separator and cathode additive.

Representative charge-discharge curves corresponding to the four kinds of SSLSBs are shown in Fig. 1 (b, d, f, h). They can be divided into two types: single plateau and dual plateau potential profiles. When PEO-based SPEs, ionic liquid, gel electrolytes or other interfacial wetting components exist in the cell as interlayers, the charge-discharge curves exhibit dual-plateau profile similar to that in liquid Li-S batteries, even if CSEs or oxide-based ISEs are used as the solid electrolyte separator. The dual-plateau profile is indicative of the solid-liquid-solid conversion mechanism in the cathode. However, for the SSLSBs constructed with sulfide-based ISEs (Fig. 1g and h), the charge-discharge curve presents

single-plateau characteristic, indicating a distinctly different solid-solid conversion mechanism.

Therefore, it is necessary to analyze and understand the chemical-electrochemical behavior of different battery systems. In general, the differences in the compositions and charge-discharge reaction mechanism mean that the different problems should be concerned in the above-mentioned battery model systems. Specifically, for the batteries in the first three types mentioned above and illustrated in Fig. 1, it is necessary to focus on the conversion mechanism of sulfur cathodes, the behavior of polysulfide chemistry and the regulation of reaction kinetics. And for the SSLSBs assembled by sulfide-based ISEs as SE and cathode additive (type 4), more attention should be paid on interface engineering design and the electrochemical stability of anode. The specific examples will be detailedly discussed in following relevant battery systems.

In the following section, we will discuss the key scientific questions and engineering design in SSLSBs of the first three types illustrated in Fig. 1.

### 3. SSLSBs based on SPEs and CSEs

As mentioned above, SPEs exhibit important roles acting as interlayers or independent SE separators [36–38]. When the above-mentioned SEs are applied in SSLSBs, the sulfur cathodes exhibit solid-liquid-solid conversion mechanism similar to the liquid system, namely the first three types

mentioned in Fig. 1, so they are discussed together in this section.

For the S/C cathodes in the liquid Li-S batteries, the electrochemical reaction of sulfur presents a two-step conversion mechanism [39–41]. The sulfur converts into  $\text{Li}_2\text{S}_n$  ( $\text{Li}_2\text{S}_8$ ,  $\text{Li}_2\text{S}_6$  and  $\text{Li}_2\text{S}_4$ ) at the first step, and  $\text{Li}_2\text{S}_n$  ( $n \geq 4$ ) further converts to  $\text{Li}_2\text{S}_2$  and  $\text{Li}_2\text{S}$ , which represent the second step in the conversion process of sulfur. The long-chain polysulfide  $\text{Li}_2\text{S}_n$  ( $n \geq 4$ ) can be dissolved in the liquid electrolytes, thus part of the polysulfides should be transported to the anode side due to the concentration difference, and these polysulfides will be transferred back to the cathode during the next charge process. The so called “shuttle effect” will lead to the irreversible loss of active materials and the fast capacity fading of the battery.

Hence, the application of SEs is expected to suppress polysulfide shuttling and prolong the lifespan of Li-S battery [23,26,42–44]. However, with the development of characterization technology, especially the *in-situ* detection method, recent works demonstrated that polysulfides could be dissolved and diffused in the PEO-based SPEs and CSEs, in a way much similar to that in ether-based liquid electrolytes [19,20,45]. In view of the wide use of the SPEs as solid electrolytes layer and interlayer for purpose of reducing the solid-solid contact impedance, revealing the polysulfide chemistry in SPEs and CSEs-based SSLSBs is fundamental and important.

### 3.1. The “polysulfide chemistry” in SSLSBs

As shown in Fig. 1b, d and 1f, the sulfur cathodes in the SSLSBs with PEO-based SPEs or CSEs show a typical two-step reaction process, which is similar to that of liquid electrolyte system [36–38]. By heating the PEO/S +  $\text{Li}_2\text{S}$ /PEO pellets at 55 °C for 24 h, Fang et al. proved that polysulfide species are soluble in SPEs (Fig. 2a) [19]. It was further verified by X-ray photoelectron spectroscopy (XPS). They stated that it was caused by the high donor number (DN) of function groups in the polymer chains, such as the ethylene oxide (EO) unit (DN = 22) in PEO chain. Another experimental study (Fig. 2b) by Liu et al. indicated that different from the corrosion of lithium anode caused by polysulfide shuttling in liquid Li-S battery, the polysulfide could be dissolved in PEO-based SPEs and transported to the surface of lithium during the discharging process, then formed a passivation interlayer, which raised the internal impedance of the full cell (Fig. 2b) and ultimately resulted in lower utilization of sulfur in cathode and deteriorated cycling performance of the battery [20]. Using

the Li|PEO-LiTFSI-LLZTO|S cell as a platform, direct tracking of the polysulfide shuttling in PEO-based CSEs was realized via real-time optical microscope imaging by Song et al. [45]. The results showed that polysulfide could be dissolved in CSEs of PEO-LiTFSI-LLZTO, and remained in electrolyte in the following cyclic process (Fig. 2c).

In addition, the ionic conductivity of the PEO-based SPEs is too low to ensure the operation of the battery at room temperature, thus the SSLSBs using PEO-based SPE always operates at high temperature of  $\geq 60$  °C or even 80 °C to facilitate the conduction of Li-ions, but the thin and viscous-liquid-like state of PEO-based SPEs is mechanically not strong enough to suppress the growth of lithium dendrite during the cycling process.

Therefore, the formation of soluble polysulfide cannot be avoided in SSLSBs that contain PEO-based SPEs [19,20,45,46]. Despite that some studies claimed that the CSEs with inorganic ceramics can partially block the diffusion of polysulfides, the slow kinetics of sulfur conversion leads to the accumulation of polysulfide on the anode side, and eventually causes capacity attenuation during extending cyclic process.

In light of the important role in the construction of solid-solid interface, inhibiting or even eliminating the dissolution and diffusion of polysulfide in SEs that contain PEO-based SPEs is very important in the design of SSLSBs. The following approaches have been adopted to achieve this goal in SSLSBs that contain PEO-based SPEs, and it is worth noting that some of them have their origins from liquid electrolyte Li-S cells.

### 3.2. Regulation strategies for polysulfide dissolution in PEO-based SSLSBs

#### 3.2.1. Regulate the conversion of sulfur cathodes

Fang et al. reported a SSLSB using polyvinylidene fluoride (PVDF) coated sulfur as the cathode and PEO-based SPE as the SE. The *ex-situ* XPS spectra and TOF-SIMS analysis proved that there were no long-chain polysulfides ( $\text{Li}_2\text{S}_n$ ,  $n \geq 4$ ) during the discharge and charge processes [19]. Combined with the DFT calculation, they demonstrated that since the polysulfide is insoluble and unstable in PVDF polymer, the conversion mechanism is changed to ‘solid-solid’ in the PVDF-coated sulfur cathodes. As a result, the sulfur in the composite cathode is transformed to solid  $\text{Li}_2\text{S}_2$  and  $\text{Li}_2\text{S}$  directly, which leads to the better cycling performance (Fig. 3a).

Accelerating the redox kinetics of sulfur cathodes is also benefitting for the formation of sulfur species in SSLSBs. Recently, Gao et al. employed

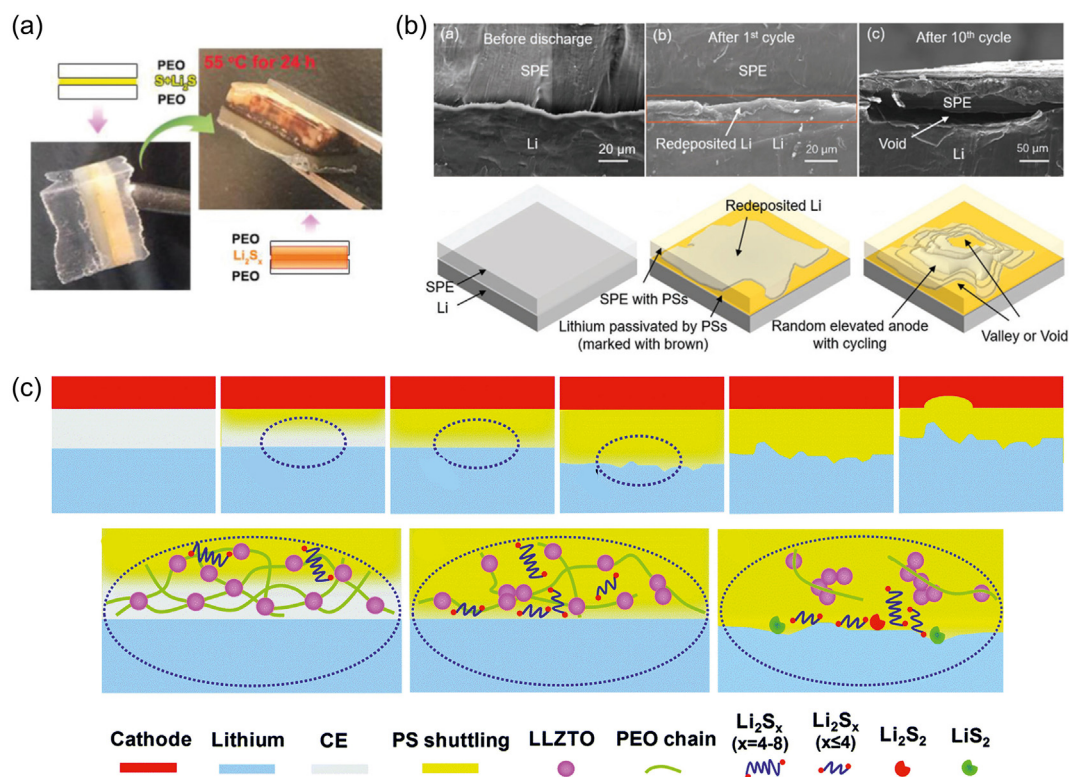


Fig. 2. The “polysulfide chemistry” in SSLSBs using PEO-based SPEs. (a) The optical images of PEO/S + Li<sub>2</sub>S/PEO pellets before and after heating at 55 °C for 24 h [19]. Reproduced with permission of Ref. [19], copyright (2020), Wiley. (b) Cross-section SEM images of the anode-electrolyte interfaces in the Li|PEO-LiTFSI|S cell at different cycle states, and the corresponding schematic illustrations of Li re-deposition process and the cell failure mechanism [20]. Reproduced with permission of Ref. [20], copyright (2021), Wiley. (c) A schematic illustration demonstrating the interfacial processes in the Li|PEO-LiTFSI-LLZTO|S cell [45]. Reproduced with permission of Ref. [45], copyright (2019), The Royal Society of Chemistry.

redox mediators (RM), which has been widely explored in liquid Li-S battery systems, to improve sulfur reaction kinetics in SSLSBs [21]. A kind of quinone-based RM 1,5-bis(2-(2-(2-methoxyethoxy)ethoxy)-ethoxy)anthra-9,10-quinone (AQT) was introduced to the cathode. When the Li<sub>2</sub>S@AQT was used to assemble SSLSBs based on PEO/LiTFSI SPEs, the oxidation of Li<sub>2</sub>S was accelerated and the utilization of active materials was improved in comparison with the bare Li<sub>2</sub>S cathode. They found that there is no thick sulfur/Li<sub>2</sub>S passivation layer formed and the soluble polysulfide species was reduced in the SPEs for the SSLSB with Li<sub>2</sub>S@AQT, which result in the improved cycling performance.

### 3.2.2. Constrain soluble polysulfides

Gao et al. prepared core-shelled Li<sub>2</sub>S@TiS<sub>2</sub> nanoparticles as the cathode materials in the SSLSB using polyimide film supported PEO/LiTFSI (PI@PEO/LiTFSI) as the solid electrolyte [22]. They demonstrated that the generated polysulfide during discharge process can be confined inside the TiS<sub>2</sub> layer due to the strong interaction between TiS<sub>2</sub> and polysulfides, thus avoiding the

dissolution in PEO-based SPEs, which is proved by the *in-situ* X-ray absorption testing and *in-situ* optical microscopic characterization (Fig. 3b, above). Besides, the redox kinetics of Li<sub>2</sub>S was accelerated by TiS<sub>2</sub> coating (Fig. 3b, below), and high energy density of 427 Wh·kg<sup>-1</sup> was achieved at a full-cell level under 80 °C.

### 3.2.3. Construct interlayers

Constructing a protecting interlayer between the cathode and the electrolyte is another way to prevent the polysulfides dissolution from the cathode. Recently, Liu et al. developed a cathode interlayer of SACNTGO-SPE (CGS) in a SSLSB [20]. The CGS interlayer was composed of super-aligned carbon nanotube (SACNT) film, graphene oxide (GO) and SPE. Since the interlayer successfully confined the polysulfides within the cathode side, the cycle performance of SPE-based was significantly improved (Fig. 3c).

### 3.2.4. Modify the anion chemistry of lithium salt

The SPEs are consisted of the polymer matrix and the dissolved lithium salts. The coordination anions of lithium salts not only are related to the ionic

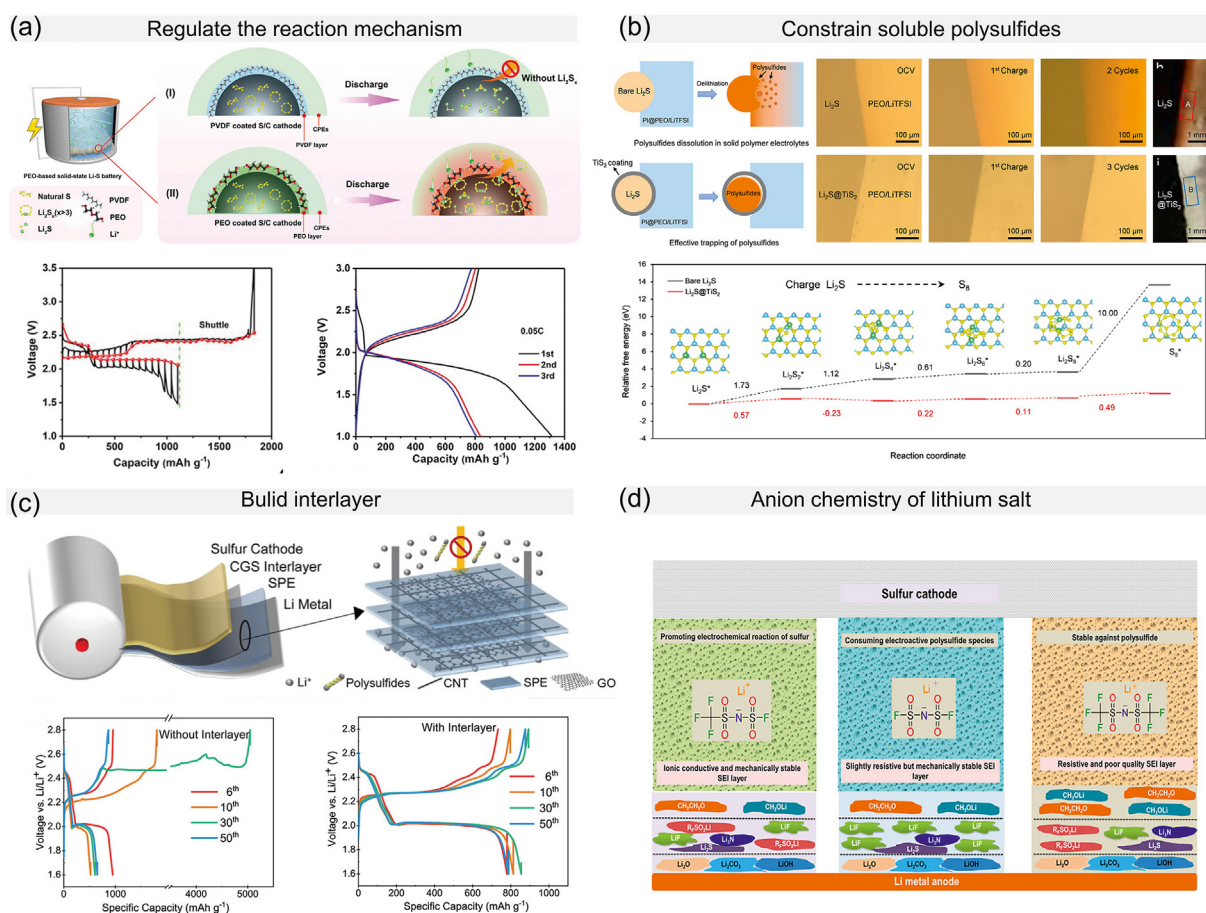


Fig. 3. The strategies reported to solve the problems induced by polysulfide dissolution in SSLSBs that contain PEO-based SPEs. (a) The schematics for the proposed mechanism and the galvanostatic intermittent titration technique (GITT) profiles of PEO-coated S/C cathode and PVDF-coated S/C cathode in PEO-based SPEs tested at 55 °C [19]. Reproduced with permission of Ref. [19], copyright (2020), Wiley. (b) The in-situ optical microscopic images (above) and the evolution process of relative free energy of the bare  $\text{Li}_2\text{S}$  and  $\text{Li}_2\text{S}@\text{TiS}_2$  cathodes at different cycles (below) [22]. Reproduced with permission of Ref. [22], copyright (2020), American Chemical Society. (c) The schematic illustration of a SPE-based SSLSB with CNT-GO-SPE cathode interlayer, and the discharge/charge profiles with and without the interlayer [20]. Reproduced with permission of Ref. [20], copyright (2021), Wiley. (d) The illustration of the SEI layer formed on Li anode with three different lithium salts [47]. Reproduced with permission of Ref. [47], copyright (2018), American Chemical Society.

conductivity and electrochemical stability of SPEs, but also take part in the formation of interfacial layer against electrodes, and may also alter the conversion dynamics of sulfur cathodes. Various works have exerted much efforts in the optimization of the anion of lithium salts in the SSLSBs that contain PEO-based SPEs recently [47–51]. In addition to the most widely used lithium bis(trifluoromethanesulfonyl)imide (LiTFSI), lots of lithium salts such as bis(fluorosulfonyl)imide (LiFSI), (fluorosulfonyl)(trifluoromethanesulfonyl)imide (LiFTFSI), (difluoromethanesulfonyl)(trifluoromethanesulfonyl)imide (LiDFTFSI) were applied to prepare PEO-based SPEs, in search for robust solid electrolyte interphase (SEI) on the lithium side (Fig. 3d), thereby to improve the cycle performance of the SSLSBs [47]. The lithium salt of LiFSI was also applied in CSEs. Judez et al.

assembled a SSLSB with  $\text{Al}_2\text{O}_3$  and LICGC filled LiFSI/PEO bilayer electrolytes [49]. Besides, the electrolyte additive of lithium azide ( $\text{LiN}_3$ ) in PEO-LiFSI SPEs can result in the formation of superior passivation layer and further enhance the cycling performance of SSLSBs [48].

#### 4. The SSLSBs based on sulfide ISEs

In contrast to the SPEs and CSEs, SSLSBs with sulfide-based ISEs exhibit shuttling effect-free electrochemical behavior due to the insolubility of polysulfide in the sulfide-based ISEs. Typically, SSLSBs with sulfide-based ISEs were assembled in a model cell under high pressure to ensure the intimate solid-solid contact, in which the active materials were mixed with SEs and conductive agents to form a composite cathode, and Li metal was used as the anode. However, SSLSBs with

sulfide-based ISEs suffer from intractable interfacial issues, including the chemo-mechanical failure and the electrochemical degradation both within the composite cathode and the electrode-electrolyte interfaces during the extending cycles [52–55].

#### 4.1. The main failure mechanism in SSLSBs based on sulfide-based ISEs

The history of SSLSBs based on sulfide-based ISEs can be traced back to 2004, in which Nobuya et al. firstly reported a SSLSB with sulfur as the active materials [26]. Subsequently, Hayashi et al. extended the cathodes in this SSLSB system from sulfur to  $\text{Li}_2\text{S}$  [23]. However, all of the above-mentioned works exhibited decent reversible specific capacity but unsatisfactory cycle performances [23,26,44]. The two main reasons were as follows: one was the sluggish conversion kinetic of the SSLSBs caused by poor ionic and electronic conductivities of sulfur or  $\text{Li}_2\text{S}$  cathodes, and the other was the volume change during discharge and charge processes. For these reasons, fresh solid-solid interface would be continuously exposed in each cycle, which led to the solid-solid contact deteriorating, and capacity fading and the chemo-mechanical failure in the cathode. Besides, the chemo-mechanical failure caused by increased stress/strain also existed in both the electrode and the electrolyte at a full-cell level.

Owing to the requirement of building efficient ionic-electronic conductive network and improving the utilization of active materials, strategies such as minishing the particle size and uniform mixing in solution processing are generally used to prepare composite cathodes [54]. These mentioned processes would bring risk for electrolyte degradation because of the weak electrochemical stability. Recently, Saneyuki Ohno et al. studied the irreversible electrolyte degradation caused by the ball milling and the cut-off potentials comprehensively taking the SSLSB of  $\text{Li-In}|\text{Li}_6\text{PS}_5\text{Cl}|\text{Li}_6\text{PS}_5\text{Cl-S-Carbon}$  as a model battery system [54]. They demonstrated that the cycle stability of SSLSBs can be successfully enhanced by balancing between the attainable capacity and effective carrier transport. Besides the degradation within the composite cathodes, continuous electrochemical degradations are also presented in electrode-electrolyte interfaces.

To improve the electrochemical performance of SSLSBs with sulfide-based ISEs, major efforts are devoted and the following three approaches can be summarized (Fig. 4): (1) Construct the composite cathode that can enhance the ionic and electronic transports, and alleviate the volume

change caused by charge and discharge [56–63]; (2) Develop functional sulfide-based ISEs with high chemical and electrochemical stabilities [64–66]; (3) Design dynamically stable electrode-electrolyte interface [18,25,32–34,67]. The first approach emphasizes the relieving of chemo-mechanical failure by the construction of composite cathode, while the other two approaches focus on realizing electrochemically stable electrode-solid electrolyte interface. The relevant works in recent years are discussed in the sections 4.2 and 4.3, and the design at the full-cell level is discussed in the section 4.4.

#### 4.2. The construction of composite cathode

To enhance the utilization of active material and the cycling stability of SSLSBs, Liang and the co-workers prepared core-shell structured  $\text{Li}_2\text{S-Li}_3\text{PS}_4$  nanoparticles with an ionic conductivity of  $10^{-7} \text{ S}\cdot\text{cm}^{-1}$ , which is much higher than that of the pristine  $\text{Li}_2\text{S}$  nanoparticles ( $10^{-13} \text{ S}\cdot\text{cm}^{-1}$ ) [60]. Excellent cycling performance of sulfide-based SSLSBs was achieved when  $\text{Li}_2\text{S-Li}_3\text{PS}_4$  nanoparticles are used in the cathode. Furthermore, Han et al. fabricated a  $\text{Li}_2\text{S-Li}_6\text{PS}_5\text{Cl-C}$  nanocomposite, in which the  $\text{Li}_2\text{S}$  and the catholyte ( $\text{Li}_6\text{PS}_5\text{Cl}$ ) are uniformly distributed in a carbon skeleton (Fig. 4a) [61]. The corresponding SSLSB ( $\text{Li-In}|\text{80Li}_2\text{S}\cdot\text{20P}_2\text{S}_5|\text{Li}_2\text{S-Li}_6\text{PS}_5\text{Cl-C}$ ) showed a high utilization of the active material and stable cycling performance at room-temperature. Yan et al. also realized high capacity and long cycle life SSLSB by using a  $\text{Li}_2\text{S@C}$  nanocomposite as the cathode active materials, which was synthesized via combusting lithium metal with  $\text{CS}_2$  (Fig. 4b) [62]. Jiang et al. fabricated  $\text{Li}_2\text{S-carbon}$  nanotube (CNT) nanocomposites by depositing the  $\text{Li}_2\text{S}$  nanoparticles on the surface of CNT surface. The resulting  $\text{Li}|\text{Li}_2\text{S-P}_2\text{S}_5\text{-P}_2\text{O}_5\text{+Li}_{10}\text{GeP}_2\text{S}_{12}|\text{Li}_2\text{S-CNT@Li}_{10}\text{GeP}_2\text{S}_{12}\text{@AB}$  SSLSB showed superior cycle performance because of the improved ionic and electronic conductivities of the cathode (Fig. 4c) [57]. Zhao et al. prepared a sulfur/ $\text{Nb}_{18}\text{W}_{16}\text{O}_{93}$ /carbon nanotubes (S/NWO/CNTs) hybrid cathode, which can achieve efficient ionic/electronic transport and promote the conversion kinetic of sulfur during charge and discharge processes. At the same time, the CNTs in the hybrid cathode can increase the electronic conductivity and suppress the volumetric change caused by the phase conversion of sulfur (Fig. 4d) [56].

These results indicated that rational design of nanocomposite structure plays a key role in accommodating the volume change and enhancing the electronic conductivity of the cathode.

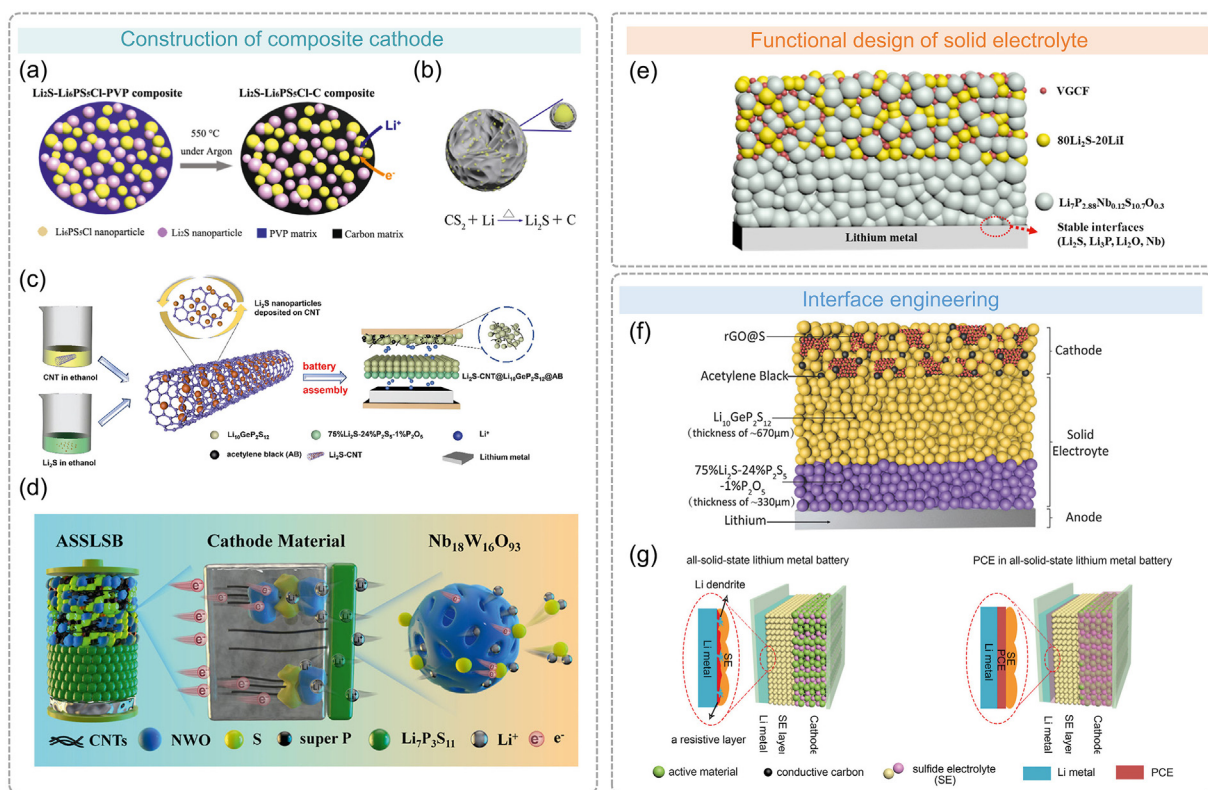


Fig. 4. The strategies reported in SSLSBs for constructing composite cathodes and optimizing electrode-electrolyte interfaces based on sulfide-based ISEs. (a) Schematic of the synthesis for the mixed conducting  $\text{Li}_2\text{S-Li}_4\text{PS}_4\text{Cl-C}$  nanocomposite [61], and (b) a  $\text{Li}_2\text{S@C}$  nanocomposite with  $\text{Li}_2\text{S}$  nanocrystals embedded in conductive carbon matrix [62]. Reproduced with permission of Ref. [61], copyright (2016), American Chemical Society. Reproduced with permission of Ref. [62], copyright (2019), American Chemical Society. (c) Schematic for preparing the  $\text{Li}_2\text{S-CNT@Li}_{10}\text{GeP}_2\text{S}_{12}\text{@AB}$  cathode [57]. Reproduced with permission of Ref. [57], copyright (2021), American Chemical Society. (d) The conversion mechanism of sulfur in the composite cathode of S/NWO/CNT [56]. Reproduced with permission of Ref. [56], copyright (2022), American Chemical Society. (e) Diagrammatic sketch of the  $\text{Li}||\text{Li}_2\text{S}$  SSLSB with  $\text{Li}_7\text{P}_{2.88}\text{Nb}_{0.12}\text{S}_{10.7}\text{O}_{0.3}$  SEs [65]. Reproduced with permission of Ref. [65], copyright (2020), American Chemical Society. (f) Schematic diagram of the SSLSB with bilayer sulfide-based ISEs [18], and (g) SSLSBs without and with the plastic crystal electrolytes (PCE) interlayer [32]. Reproduced with permission of Ref. [18], copyright (2017), John Wiley and Sons. Reproduced with permission of Ref. [32], copyright (2019), Wiley.

#### 4.3. Design of stable anode-electrolyte interface

Except for several relatively stable sulfide-based ISEs such as  $\text{Li}_3\text{PS}_4$  and  $\text{Li}_2\text{S-P}_2\text{S}_5\text{-P}_2\text{O}_5$  glass ceramic, the majority of sulfide-based ISEs are unstable against the lithium metal, which hinders its application in SSLSBs with high specific energy. To improve the dynamical stability of sulfide-ISE, strategies such as the functional structure design of SEs and construction of dynamically stable interlayer were adapted [64–66]. Jiang et al. developed a novel solid electrolyte of  $\text{Li}_7\text{P}_{2.88}\text{Nb}_{0.12}\text{S}_{10.7}\text{O}_{0.3}$  with an improved electrochemical stability and a high room temperature ionic conductivity of  $3.59\text{ mS}\cdot\text{cm}^{-1}$  [65]. Due to the co-doping of Nb and O based on  $\text{Li}_7\text{P}_3\text{S}_{11}$ , Nb,  $\text{Li}_2\text{S}$ ,  $\text{Li}_3\text{P}$  and  $\text{Li}_2\text{O}$  can be formed at the surface of the lithium anode during the charge-discharge process, which promote the uniform deposition of Li and inhibit the further occurrence of side reactions, eventually improve the cycle and rate performances of the SSLSBs (Fig. 4e).

Constructing an interlayer is essential to enhancing the dynamic stability of the electrode-electrolyte interfaces [18,25,32–34,67]. A double-layered design is a commonly used strategy in sulfide-based ISEs separators [18,68]. For example,  $\text{Li}_3\text{PS}_4$  and  $\text{Li}_2\text{S-P}_2\text{S}_5\text{-P}_2\text{O}_5$  glass ceramic are often used at the anode side and brought into contact with lithium metal to take advantage of the formation of ionic-conductive but electronic-insulative interphase. A different electrolyte such as  $\text{Li}_{10}\text{GeP}_2\text{S}_{12}$  is adopted in the cathode side to ensure high ion transport. Yao et al. used  $\text{Li}_2\text{S-P}_2\text{S}_5\text{-P}_2\text{O}_5$  glass ceramic thin pellet as the interlayer to achieve an electrochemically stable interface in the anode side of SSLSBs. As shown in Fig. 4f, using bilayer electrolytes composed of  $\text{Li}_{10}\text{GeP}_2\text{S}_{12}$  and  $\text{Li}_2\text{S-P}_2\text{S}_5\text{-P}_2\text{O}_5$  glass ceramic, the SSLSB exhibited a high specific capacity of  $830\text{ mAh}\cdot\text{g}^{-1}$  after 750 cycles at a current density of  $1\text{ C}$  and  $60\text{ }^\circ\text{C}$ , indicating excellent long-term cycling stability [18].

Plastic crystal electrolyte (PCE) was also introduced to optimize interface contact and improve electrochemical stability in the recent year [69–72]. For example, Sun et al. adopted the PCE as the interlayer to solve the interfacial instability problem in  $\text{Li}_{10}\text{GeP}_2\text{S}_{12}$  electrolyte [32]. They stated that the PCE interlayer can prevent the direct contact between LGPS and Li metal, and enhance the kinetics of the battery, leading to significant progress towards achieving high energy density SSLSBs (Fig. 4g). As a result, SSLSB based on polyacrylonitrile-sulfur (PAN-S) composite cathode exhibited an initial specific capacity of  $1682 \text{ mAh}\cdot\text{g}^{-1}$  (based on sulfur). The specific capacity of the second discharge is  $890 \text{ mAh}\cdot\text{g}^{-1}$ , and after 100 cycles, it remained at  $775 \text{ mAh}\cdot\text{g}^{-1}$  at a current density of  $0.13 \text{ mA}\cdot\text{cm}^{-2}$ .

Alloy anode (such as Li-In alloy, Li-Al alloy or Li-Ge alloy) is another approach to improve the stability of the anode-electrolyte interface [25,34,35]. Li-In alloy is widely used in SSLSBs with sulfide-based ISEs due to fast diffusion of Li atom in indium anode, which can effectively avoid the growth of Li dendrite at a relatively high current density [35].

#### 4.4. Other aspects

These recent studies show that electrochemical performance of SSLSBs with sulfide-based ISEs can be significantly improved by rational design in the structure of composite cathodes and the interfacial engineering in the enhancement of the solid-solid contact. However, from the view of practical application, more technical aspects need to be considered. Firstly, the poor air-stability of sulfide-based ISEs means that they often need to be fabricated in high purity argon gloved box, which makes the production and application more complex and expensive. Secondly, sulfide-based ISEs suffer from high areal impedance and relatively high mass ratio in full cells due to their rigid ceramic nature, which will limit the energy density and power density of the SSLSBs. Last but not least, SSLSBs with sulfide-based ISEs are usually assembled under pressures over 200 MPa and operated under pressures over 60 MPa, to ensure the intimate solid-solid contact [18,53,60]. Such high pressure demands bring serious challenges in practical applications. The innovation of key materials and comprehensive understanding of the failure mechanism may help to promote the R&D process of high energy density and long cycling SSLSBs with sulfide-based ISEs.

## 5. Conclusions and perspectives

In this review, we summarized recent advances in SSLSBs including material development, interfacial modification, and mechanistic investigations.

With these efforts, SSLSBs with high specific capacity (ca.  $1500 \text{ mAh}\cdot\text{g}^{-1}$ ) and long lifespan (ca. 700 cycles) can be achieved in some specific systems at electrodes level [18,51,62]. But for most reported SSLSBs, the full-cell-level energy densities are still no more than  $100 \text{ Wh}\cdot\text{kg}^{-1}$  even though many of them operate under  $60^\circ\text{C}$  [68]. Such performance is far inferior to that of the liquid Li-S cells or commercial Li-ion batteries [2,4]. This could be attributed to low active materials loading and high mass ratio of solid electrolytes, as well as the Li dendrite growth limiting the lifespan of SSLSBs. It is worth mentioning that the highest energy density of room-temperature solid-state Li-S battery can reach  $370.6 \text{ Wh}\cdot\text{kg}^{-1}$  with high loading of active materials ( $\text{Li}_2\text{S}$ :  $7.64 \text{ mg}\cdot\text{cm}^{-2}$ ) and thin  $\text{Li}_3\text{PS}_4$  electrolyte layer (ca.  $100 \mu\text{m}$ ), but it can only cycle for about 20 cycles at a rate of 0.05 C. This indicates that SSLSBs with high energy density are achievable [73].

Further development of SSLSBs requires more fundamental understanding of the electrochemical processes in the cells, so as to promote the cycle performance of SSLSBs. The strongly recommended future efforts are summarized in Fig. 5 and detailed in the following.

*High loading solid cathode.* To improve the energy density, it is necessary to increase the active materials loading to more than  $6 \text{ mg}\cdot\text{cm}^{-2}$ , and reduce the proportion of catholyte and conductive agents to less than 50% in solid-state composite cathodes. Therefore, it is important to construct efficient ionic and electronic conducting networks. Except for the use of special high-pressure dies, innovative binders that can accommodate the dynamic volume change or SPEs with large elastic modulus may help to resolve these challenges. In addition, the cathode material could be specifically designed to suit the needs in solid-state cathodes. For example, solid-solid conversion can be realized and no polysulfide is produced during charge and discharge processes for organic sulfur cathode materials, which has great advantages in SSLSBs [32,74–77]. For the small number of reported SSLSBs involving organic sulfur cathodes, the SE layers used were mainly sulfide-based ISEs [32,74,75]. Extending the SEs to SPEs and CSEs as well as the related mechanisms are worth investigating in the future.

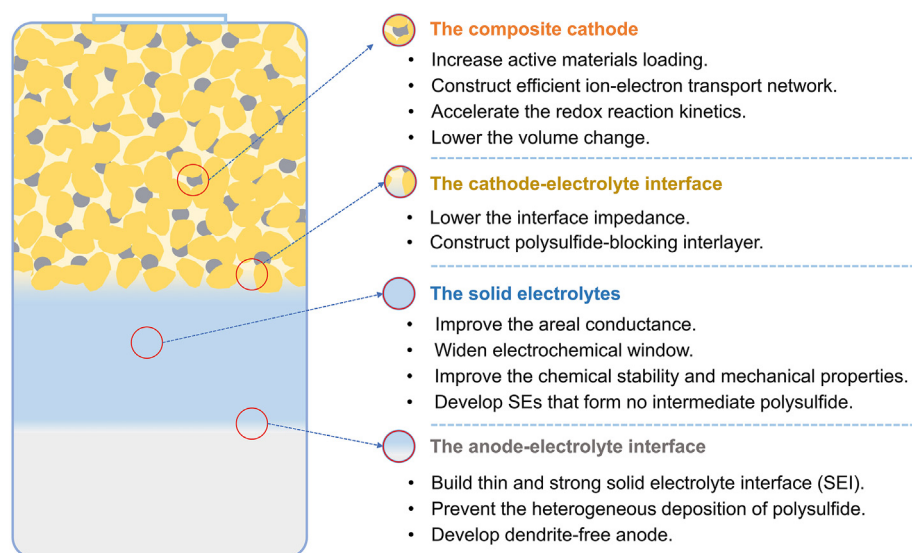


Fig. 5. Efforts should be made to furtherly improve the performance of SSLSBs at full-cell level.

**The electrode-electrolyte interface.** It is very important to reduce contact impedance and improve electrochemical stability in solid-state battery system. For this goal, efforts should be made to prevent polysulfide dissolution at the cathode side and the heterogeneous deposition of polysulfide at the anode side. Construction of polysulfide-blocking interlayers at the cathode is a feasible approach. Besides, it is necessary to build thin and strong solid electrolyte interphase (SEI) or develop dendrite-free anode.

**Novel SE systems.** The SEs is the key component in solid-state batteries. The amount of SE used in the battery determines the energy density of the battery to a large extent once the cathode and anode active materials are selected. The conductivity of SE strongly affects the rate performance. The structure and the manufacturing process of SEs should be optimized to reduce the thickness of the SE separator layer (within 100  $\mu\text{m}$ ) and improve the areal ionic conductivity. Besides, applying the SEs such as sulfide-based ISEs and further developing SEs that form no intermediate polysulfide are the fundamental solutions to the dissolution and diffusion of polysulfides in SSLSBs. It is also essential to widen the electrochemical window, improve the chemical stability and mechanical properties.

Future material developments and interfacial control may eventually pave the way towards practical SSLSBs.

## Acknowledgements

This work is supported by the National Key R&D Program of China (2021YFB3800300) and China Postdoctoral Science Foundation (BX20220199).

## References

- [1] Bruce P G, Freunberger S A, Hardwick L J, Tarascon J M. Li-O<sub>2</sub> and Li-S batteries with high energy storage[J]. *Nat. Mater.*, 2011, 11(1): 19–29.
- [2] Zhou G, Chen H, Cui Y. Formulating energy density for designing practical lithium-sulfur batteries[J]. *Nat. Energy*, 2022, 7(4): 312–319.
- [3] Yang X F, Li X, Adair K, Zhang H M, Sun X L. Structural design of lithium-sulfur batteries: from fundamental research to practical application[J]. *Electrochem. Energy R.*, 2018, 1(3): 239–293.
- [4] Chung S H, Manthiram A. Current status and future prospects of metal-sulfur batteries[J]. *Adv. Mater.*, 2019, 31(27): e1901125.
- [5] Huang Y, Lin L, Zhang C, Liu L, Li Y, Qiao Z, Lin J, Wei Q, Wang L, Xie Q, Peng D L. Recent advances and strategies toward polysulfides shuttle inhibition for high-performance Li-S batteries[J]. *Adv. Sci.*, 2022, 9(12): e2106004.
- [6] Yang X, Luo J, Sun X. Towards high-performance solid-state Li-S batteries: from fundamental understanding to engineering design[J]. *Chem. Soc. Rev.*, 2020, 49(7): 2140–2195.
- [7] Bonnick P, Muldoon J. The dr jekyll and Mr hyde of lithium sulfur batteries[J]. *Energy Environ. Sci.*, 2020, 13(12): 4808–4833.
- [8] Barghamadi M, Best A S, Bhatt A I, Hollenkamp A F, Musameh M, Rees R J, R  ther T. Lithium-sulfur batteries—the solution is in the electrolyte, but is the electrolyte a solution? [J]. *Energy Environ. Sci.*, 2014, 7(12): 3902–3920.
- [9] Ding B, Wang J, Fan Z J, Chen S, Lin Q Y, Lu X J, Dou H, Nanjundan A K, Yushin G, Zhang X G, Yamauchi Y. Solid-state lithium-sulfur batteries: advances, challenges and perspectives[J]. *Mater. Today*, 2020, 40: 114–131.
- [10] Pan H, Cheng Z, He P, Zhou H S. A review of solid-state lithium-sulfur battery: ion transport and polysulfide chemistry[J]. *Energy Fuel*, 2020, 34(10): 11942–11961.
- [11] Zheng Y, Yao Y Z, Ou J H, Li M, Luo D, Dou H Z, Li Z Q, Amine K, Yu A P, Chen Z W. A review of composite solid-state electrolytes for lithium batteries: fundamentals, key materials and advanced structures[J]. *Chem. Soc. Rev.*, 2020, 49(23): 8790–8839.
- [12] Zhang Q, Cao D X, Ma Y, Natan A, Aurora P, Zhu H L. Sulfide-based solid-state electrolytes: synthesis, stability,

- and potential for all-solid-state batteries[J]. *Adv. Mater.*, 2019, 31(44): e1901131.
- [13] Chen R S, Li Q H, Yu X Q, Chen L Q, Li H. Approaching practically accessible solid-state batteries: stability issues related to solid electrolytes and interfaces[J]. *Chem. Rev.*, 2020, 120(14): 6820–6877.
- [14] Li X N, Liang J W, Yang X F, Adair K R, Wang C H, Zhao F P, Sun X L. Progress and perspectives on halide lithium conductors for all-solid-state lithium batteries[J]. *Energy Environ. Sci.*, 2020, 13(5): 1429–1461.
- [15] Kamaya N, Homma K, Yamakawa Y, Hirayama M, Kanno R, Yonemura M, Kamiyama T, Kato Y, Hama S, Kawamoto K, Mitsui A. A lithium superionic conductor[J]. *Nat. Mater.*, 2011, 10(9): 682–686.
- [16] Kato Y, Hori S, Saito T, Suzuki K, Hirayama M, Mitsui A, Yonemura M, Iba H, Kanno R. High-power all-solid-state batteries using sulfide superionic conductors[J]. *Nat. Energy*, 2016, 1(4): 16030.
- [17] Manthiram A, Yu X W, Wang S F. Lithium battery chemistries enabled by solid-state electrolytes[J]. *Nat. Rev. Mater.*, 2017, 2(4): 16103.
- [18] Yao X Y, Huang N, Han F D, Zhang Q, Wan H L, Mwizerwa J P, Wang C S, Xu X X. High-performance all-solid-state lithium-sulfur batteries enabled by amorphous sulfur-coated reduced graphene oxide cathodes[J]. *Adv. Energy Mater.*, 2017, 7(17): 1602923.
- [19] Fang R X, Xu H H, Xu B Y, Li X Y, Li Y T, Goodenough J B. Reaction mechanism optimization of solid-state Li-S batteries with a PEO-based electrolyte[J]. *Adv. Funct. Mater.*, 2020, 31(2): 2001812.
- [20] Liu Y, Liu H W, Lin Y T, Zhao Y X, Yuan H, Su Y P, Zhang J F, Ren S Y, Fan H Y, Zhang Y G. Mechanistic investigation of polymer-based all-solid-state lithium-sulfur battery[J]. *Adv. Funct. Mater.*, 2021, 31(41): 2104863.
- [21] Gao X, Zheng X L, Tsao Y C, Zhang P, Xiao X, Ye Y S, Li J, Yang Y F, Xu R, Bao Z N, Cui Y. All-solid-state lithium-sulfur batteries enhanced by redox mediators[J]. *J. Am. Chem. Soc.*, 2021, 143(43): 18188–18195.
- [22] Gao X, Zheng X, Wang J, Zhang Z, Xiao X, Wan J, Ye Y, Chou L Y, Lee H K, Wang J, Vilá R A, Yang Y, Zhang P, Wang L W, Cui Y. Incorporating the nanoscale encapsulation concept from liquid electrolytes into solid-state lithium-sulfur batteries[J]. *Nano Lett.*, 2020, 20(7): 5496–5503.
- [23] Hayashi A, Ohtsubo R, Ohtomo T, Mizuno F, Tatsumisago M. All-solid-state rechargeable lithium batteries with  $\text{Li}_2\text{S}$  as a positive electrode material[J]. *J. Power Sources*, 2008, 183(1): 422–426.
- [24] Wan H L, Zhang B, Liu S F, Zhang J X, Yao X Y, Wang C S. Understanding  $\text{LiI-LiBr}$  catalyst activity for solid state  $\text{Li}_2\text{S/S}$  reactions in an all-solid-state lithium battery[J]. *Nano Lett.*, 2021, 21(19): 8488–8494.
- [25] Pan H, Zhang M H, Cheng Z, Jiang H Y, Yang J G, Wang P F, He P, Zhou H S. Carbon-free and binder-free  $\text{Li-Al}$  alloy anode enabling an all-solid-state Li-S battery with high energy and stability[J]. *Sci. Adv.*, 2022, 8(15): 4372.
- [26] Machida N, Kobayashi K, Nishikawa Y, Shigematsu T. Electrochemical properties of sulfur as cathode materials in a solid-state lithium battery with inorganic solid electrolytes[J]. *Solid State Ionics*, 2004, 175(1–4): 247–250.
- [27] Ulissi U, Ito S, Hosseini S M, Varzi A, Aihara Y, Passerini S. High capacity all-solid-state lithium batteries enabled by pyrite-sulfur composites[J]. *Adv. Energy Mater.*, 2018, 8(26): 1801462.
- [28] Long P, Xu Q, Peng G, Yao X Y, Xu X X. NiS nanorods as cathode materials for all-solid-state lithium batteries with excellent rate capability and cycling stability[J]. *Chem. electrochem*, 2016, 3(5): 764–769.
- [29] Zhang Q, Ding Z G, Liu G Z, Wan H L, Mwizerwa J P, Wu J H, Yao X Y. Molybdenum trisulfide based anionic redox driven chemistry enabling high-performance all-solid-state lithium metal batteries[J]. *Energy Storage Mater.*, 2019, 23: 168–180.
- [30] Yao X Y, Liu D, Wang C S, Long P, Peng G, Hu Y S, Li H, Chen L Q, Xu X X. High-energy all-solid-state lithium batteries with ultralong cycle life[J]. *Nano Lett.*, 2016, 16(11): 7148–7154.
- [31] Shin B R, Nam Y J, Kim J W, Lee Y G, Jung Y S. Interfacial architecture for extra  $\text{Li}^+$  storage in all-solid-state lithium batteries[J]. *Sci. Rep.*, 2014, 4: 5572.
- [32] Wang C H, Adair K R, Liang J W, Li X N, Sun Y P, Li X, Wang J W, Sun Q, Zhao F P, Lin X T, Li R Y, Huang H, Zhang L, Yang R, Lu S G, Sun X L. Solid-state plastic crystal electrolytes: effective protection interlayers for sulfide-based all-solid-state lithium metal batteries[J]. *Adv. Funct. Mater.*, 2019, 29(26): 1900392.
- [33] Wan H L, Liu S F, Deng T, Xu J J, Zhang J X, He X Z, Ji X, Yao X Y, Wang C S. Bifunctional interphase-enabled  $\text{Li}_{10}\text{GeP}_2\text{S}_{12}$  electrolytes for lithium-sulfur battery[J]. *ACS Energy Lett.*, 2021, 6(3): 862–868.
- [34] Yi J, Chen L, Liu Y, Geng H, Fan L Z. High capacity and superior cyclic performances of all-solid-state lithium-sulfur batteries enabled by a high-conductivity  $\text{Li}_{10}\text{SnS}_2\text{S}_{12}$  solid electrolyte[J]. *ACS Appl. Mater. Interfaces*, 2019, 11(40): 36774–36781.
- [35] Wan J, Song Y X, Chen W P, Guo H J, Shi Y, Guo Y J, Shi J L, Guo Y G, Jia F F, Wang F Y, Wen R, Wan L J. Micromechanism in all-solid-state alloy-metal batteries: regulating homogeneous lithium precipitation and flexible solid electrolyte interphase evolution[J]. *J. Am. Chem. Soc.*, 2021, 143(2): 839–848.
- [36] Wang L, Yin X, Jin C, Lai C, Qu G, Zheng G W. Cathode-supported-electrolyte configuration for high-performance all-solid-state lithium-sulfur batteries[J]. *ACS Appl. Energy Mater.*, 2020, 3(12): 11540–11547.
- [37] Tao X, Liu Y, Liu W, Zhou G, Zhao J, Lin D, Zu C, Sheng O, Zhang W, Lee H W, Cui Y. Solid-State Lithium-sulfur batteries operated at 37 °C with composites of nanostructured  $\text{Li}_7\text{La}_3\text{Zr}_2\text{O}_{12}$ /carbon foam and polymer[J]. *Nano Lett.*, 2017, 17(5): 2967–2972.
- [38] Wang Q S, Wen Z Y, Jin J, Guo J, Huang X, Yang J H, Chen C H. A gel-ceramic multi-layer electrolyte for long-life lithium sulfur batteries[J]. *Chem. Commun.*, 2016, 52(8): 1637–1640.
- [39] Busche M R, Adelhelm P, Sommer H, Schneider H, Leitner K, Janek J. Systematical electrochemical study on the parasitic shuttle-effect in lithium-sulfur-cells at different temperatures and different rates[J]. *J. Power Sources*, 2014, 259: 289–299.
- [40] Kumaresan K, Mikhaylik Y, White R E. A mathematical model for a lithium-sulfur cell[J]. *J. Electrochem. Soc.*, 2008, 155(8): A576–A582.
- [41] Mikhaylik Y V, Akridge J R. Polysulfide shuttle study in the  $\text{Li/S}$  battery system[J]. *J. Electrochem. Soc.*, 2004, 151(11): A1969.
- [42] Hassoun J, Scrosati B. A high-performance polymer tin sulfur lithium ion battery[J]. *Angew. Chem. Int. Ed.*, 2010, 49(13): 2371–2374.
- [43] Jeong S S, Lim Y T, Choi Y J, Cho G B, Kim K W, Ahn H J, Cho K K. Electrochemical properties of lithium sulfur cells using PEO polymer electrolytes prepared under three different mixing conditions[J]. *J. Power Sources*, 2007, 174(2): 745–750.
- [44] Kobayashi T, Imade Y, Shishihara D, Homma K, Nagao M, Watanabe R, Yokoi T, Yamada A, Kanno R, Tatsumi T. All

- solid-state battery with sulfur electrode and thio-lisicon electrolyte[J]. *J. Power Sources*, 2008, 182(2): 621–625.
- [45] Song Y X, Shi Y, Wan J, Lang S Y, Hu X C, Yan H J, Liu B, Guo Y G, Wen R, Wan L J. Direct tracking of the polysulfide shuttling and interfacial evolution in all-solid-state lithium-sulfur batteries: a degradation mechanism study[J]. *Energy Environ. Sci.*, 2019, 12(8): 2496–2506.
- [46] Wang L, Yin X, Li B, Zheng G W. Mixed ionically/electronically conductive double-phase interface enhanced solid-state charge transfer for a high-performance all-solid-state Li-S battery[J]. *Nano Lett.*, 2022, 22(1): 433–440.
- [47] Eshetu G G, Judez X, Li C, Martinez-Ibanez M, Gracia I, Bondarchuk O, Carrasco J, Rodriguez-Martinez L M, Zhang H, Armand M. Ultrahigh performance all solid-state lithium sulfur batteries: salt anion's chemistry-induced anomalous synergistic effect[J]. *J. Am. Chem. Soc.*, 2018, 140(31): 9921–9933.
- [48] Eshetu G G, Judez X, Li C, Bondarchuk O, Rodriguez-Martinez L M, Zhang H, Armand M. Lithium azide as an electrolyte additive for all-solid-state lithium-sulfur batteries[J]. *Angew. Chem. Int. Ed.*, 2017, 56(48): 15368–15372.
- [49] Judez X, Zhang H, Li C, Eshetu G G, Zhang Y, González-Marcos J A, Armand M, Rodriguez-Martinez L M. Polymer-rich composite electrolytes for all-solid-state Li-S cells [J]. *J. Phys. Chem. Lett.*, 2017, 8(15): 3473–3477.
- [50] Judez X, Zhang H, Li C, Gonzalez-Marcos J A, Zhou Z, Armand M, Rodriguez-Martinez L M. Lithium bis(-fluorosulfonyl)imide/poly(ethylene oxide) polymer electrolyte for all solid-state Li-S cell[J]. *J. Phys. Chem. Lett.*, 2017, 8(9): 1956–1960.
- [51] Zhang H, Oteo U, Judez X, Eshetu G G, Martinez-Ibañez M, Carrasco J, Li C, Armand M. Designer anion enabling solid-state lithium-sulfur batteries[J]. *Joule*, 2019, 3(7): 1689–1702.
- [52] Chinnam P R, Xu L, Cai L, Cordes N L, Kim S, Efav C M, Murray D J, Dufek E J, Xu H, Li B. Unlocking failure mechanisms and improvement of practical Li-S pouch cells through in operando pressure study[J]. *Adv. Energy Mater.*, 2021, 12(7): 2103048.
- [53] Ohno S, Koerver R, Dewald G, Rosenbach C, Titscher P, Steckermeier D, Kwade A, Janek J, Zeier W G. Observation of chemomechanical failure and the influence of cut off potentials in all-solid-state Li-S batteries[J]. *Chem. Mater.*, 2019, 31(8): 2930–2940.
- [54] Ohno S, Rosenbach C, Dewald G F, Janek J, Zeier W G. Linking solid electrolyte degradation to charge carrier transport in the thiophosphate-based composite cathode toward solid-state lithium-sulfur batteries[J]. *Adv. Funct. Mater.*, 2021, 31(18): 2010620.
- [55] Lewis J A, Tippens J, Cortes F J Q, McDowell M T. Chemo-mechanical challenges in solid-state batteries[J]. *Trends Chem.*, 2019, 1(9): 845–857.
- [56] Zhao B S, Wang L, Liu S, Li G R, Gao X P. High-efficiency hybrid sulfur cathode based on electroactive niobium tungsten oxide and conductive carbon nanotubes for all-solid-state lithium-sulfur batteries[J]. *ACS Appl. Mater. Interfaces*, 2022, 14(1): 1212–1221.
- [57] Jiang M, Liu G, Zhang Q, Zhou D, Yao X. Ultrasmall Li<sub>2</sub>S-carbon nanotube nanocomposites for high-rate all-solid-state lithium-sulfur batteries[J]. *ACS Appl. Mater. Interfaces*, 2021, 13(16): 18666–18672.
- [58] Yamamoto M, Goto S, Tang R, Nomura K, Hayasaka Y, Yoshioka Y, Ito M, Morooka M, Nishihara H, Kyotani T. Nano-confinement of insulating sulfur in the cathode composite of all-solid-state Li-S batteries using flexible carbon materials with large pore volumes[J]. *ACS Appl. Mater. Interfaces*, 2021, 13(32): 38613–38622.
- [59] Yue J, Huang Y L, Liu S F, Chen J, Han F D, Wang C S. Rational designed mixed-conductive sulfur cathodes for all-solid-state lithium batteries[J]. *ACS Appl. Mater. Interfaces*, 2020, 12(32): 36066–36071.
- [60] Lin Z, Liu Z C, Dudney N J, Liang C D. Lithium superionic sulfide cathode for all-solid lithium-sulfur batteries[J]. *ACS Nano*, 2013, 7(3): 2829–2833.
- [61] Han F D, Yue J, Fan X L, Gao T, Luo C, Ma Z H, Suo L M, Wang C S. High-performance all-solid-state lithium-sulfur battery enabled by a mixed-conductive Li<sub>2</sub>S nanocomposite [J]. *Nano Lett.*, 2016, 16(7): 4521–4527.
- [62] Yan H F, Wang H C, Wang D H, Li X, Gong Z L, Yang Y. *In situ* generated Li<sub>2</sub>S-C nanocomposite for high-capacity and long-life all-solid-state lithium sulfur batteries with ultrahigh areal mass loading[J]. *Nano Lett.*, 2019, 19(5): 3280–3287.
- [63] Hakari T, Fujita Y, Deguchi M, Kawasaki Y, Otoyama M, Yoneda Y, Sakuda A, Tatsumisago M, Hayashi A. Solid electrolyte with oxidation tolerance provides a high-capacity Li<sub>2</sub>S-based positive electrode for all-solid-state Li/S batteries[J]. *Adv. Funct. Mater.*, 2021, 32(5): 2106174.
- [64] Jiang Z, Li Z X, Wang X L, Gu C D, Xia X H, Tu J P. Robust Li<sub>6</sub>PS<sub>5</sub>I interlayer to stabilize the tailored electrolyte Li<sub>9.95</sub>SnP<sub>2</sub>S<sub>11.95</sub>F<sub>0.05</sub>/Li metal interface[J]. *ACS Appl. Mater. Inter.*, 2021, 13(26): 30739–30745.
- [65] Jiang Z, Liang T B, Liu Y, Zhang S Z, Li Z X, Wang D H, Wang X L, Xia X H, Gu C D, Tu J P. Improved ionic conductivity and Li dendrite suppression capability toward Li<sub>7</sub>P<sub>3</sub>S<sub>11</sub>-based solid electrolytes triggered by Nb and O cosubstitution [J]. *ACS Appl. Mater. Inter.*, 2020, 12(49): 54662–54670.
- [66] Zhou L, Tufail M K, Ahmad N, Song T, Chen R, Yang W. Strong interfacial adhesion between the Li<sub>2</sub>S cathode and a functional Li<sub>7</sub>P<sub>2.9</sub>Ce<sub>0.2</sub>S<sub>10.9</sub>Cl<sub>0.3</sub> solid-state electrolyte endowed long-term cycle stability to all-solid-state lithium-sulfur batteries[J]. *ACS Appl. Mater. Inter.*, 2021, 13(24): 28270–28280.
- [67] Wang S, Zhang Y, Zhang X, Liu T, Lin Y H, Shen Y, Li L, Nan C W. High-conductivity argyrodite Li<sub>6</sub>P<sub>5</sub>Cl solid electrolytes prepared via optimized sintering processes for all-solid-state lithium-sulfur batteries[J]. *ACS Appl. Mater. Inter.*, 2018, 10(49): 42279–42285.
- [68] Wu J H, Liu S F, Han F D, Yao X Y, Wang C S. Lithium/sulfide all-solid-state batteries using sulfide electrolytes[J]. *Adv. Mater.*, 2020, 33(6): 2000751.
- [69] Gao H C, Xue L G, Xin S, Park K, Goodenough J B. A plastic-crystal electrolyte interphase for all-solid-state sodium batteries[J]. *Angew. Chem. Int. Ed.*, 2017, 56(20): 5541–5545.
- [70] Chen S J, Zhang J X, Nie L, Hu X C, Huang Y Q, Yu Y, Liu W. All-solid-state batteries with a limited lithium metal anode at room temperature using a garnet-based electrolyte[J]. *Adv. Mater.*, 2021, 33(1): 2002325.
- [71] Wang J, Huang G, Chen K, Zhang X B. An adjustable-porosity plastic crystal electrolyte enables high-performance all-solid-state lithium-oxygen batteries[J]. *Angew. Chem. Int. Ed.*, 2020, 59(24): 9382–9387.
- [72] Alarco P J, Abu-Lebdeh Y, Abouimrane A, Armand M. The plastic-crystalline phase of succinonitrile as a universal matrix for solid-state ionic conductors[J]. *Nat. Mater.*, 2004, 3(7): 476–481.
- [73] Xu R C, Yue J, Liu S F, Tu J P, Han F D, Liu P, Wang C S. Cathode-supported all-solid-state lithium-sulfur batteries with high cell-level energy density[J]. *ACS Energy Lett.*, 2019, 4(5): 1073–1079.
- [74] Hao F, Liang Y L, Zhang Y, Chen Z Y, Zhang J B, Ai Q, Guo H, Fan Z, Lou J, Yao Y. High-energy all-solid-state organic-lithium batteries based on ceramic electrolytes[J]. *ACS Energy Lett.*, 2020, 6(1): 201–207.

- [75] Zhang Y Y, Sun Y L, Peng L F, Yang J Q, Jia H H, Zhang Z R, Shan B, Xie J. Se as eutectic accelerator in sulfurized polyacrylonitrile for high performance all-solid-state lithium-sulfur battery[J]. *Energy Storage Mater.*, 2019, 21: 287–296.
- [76] Dong D R, Zhou B, Sun Y F, Zhang H, Zhong G M, Dong Q Y, Fu F, Qian H, Lin Z Y, Lu D R, Shen Y B, Wu J H, Chen L W, Chen H W. Polymer electrolyte glue: a universal interfacial modification strategy for all-solid-state Li batteries[J]. *Nano Lett.*, 2019, 19(4): 2343–2349.
- [77] Sun Y F, Zhong G M, Zhao Z, Cao M, Zhou H, Zhang S J, Qian H, Lin Z Y, Lu D R, Wu J H, Chen H W. Polymeric sulfur as a Li ion conductor[J]. *Nano Lett.*, 2020, 20(3): 2191–2196.

## 固态锂硫电池综述：从硫正极转化机制到电池的工程化设计

贾欢欢<sup>a</sup>, 胡晨吉<sup>a</sup>, 张熠霄<sup>a</sup>, 陈立桅<sup>a,b,c,\*</sup>

<sup>a</sup>上海交通大学化学化工学院, 变革性分子前沿科学中心, 上海电化学能源器件工程技术研究中心, 物质科学原位中心, 上海 200240, 中国

<sup>b</sup>上海交通大学溥渊未来技术学院未来电池研究中心, 上海 200240, 中国

<sup>c</sup>中国科学院苏州纳米技术与纳米仿生研究所 i-Lab, 江苏 苏州 215123, 中国

### 摘要

锂硫电池具有超高的理论能量密度 ( $2567 \text{ Wh}\cdot\text{kg}^{-1}$ ), 且其实际能量密度最高可达  $600 \text{ Wh}\cdot\text{kg}^{-1}$ 。然而, 液态体系的 Li-S 电池和传统锂电池一样存在着安全隐患。用固态电解质取代电解液有望提高锂电池的安全性能, 在近二十年受到了广泛的研究。对于固态锂硫电池来说, 除了由于正极材料本身的不同带来的转化机制上的差别, 固态电解质的物理化学性质也会显著影响其电化学行为。这篇综述分类讨论了已报道的不同固态锂硫电池体系在性能上的优缺点及其中主要的失效机制, 对其能量密度低、循环稳定性差的原因及改善电池综合性能的策略进行了归纳分析, 旨在从固态锂硫电池微观机制到全电池水平的工程化设计提供全面的理解, 推动固态锂硫电池的进一步发展。

**关键词:** 固态锂硫电池; 转化动力学; 动力学稳定的界面; 失效机理; 工程化设计